DISSOCIATION OF ^{6}He

J. Wang[1], A. Galonsky, F. Deák[a], Á. Horváth,[a] K. Ieki[b], Y. Iwata[b2], Á. Kiss[a], J.J. Kolata[c], J. Kruse[3], H. Schelin[d], J. von Schwarzenberg[c], Z. Seres[e], E. Tryggestad, R. White-Stevens[c], R.E. Warner[f] and P. Zecher[4]

^{6}He is a good system in which to study the phenomena of dripline nuclei because of its tight α-core and because the underlying α-n interaction is well known. In our experiment a beam of ^{6}He with E/A = 25.2 MeV and intensity ~ 10^4/s was delivered to targets of U, Pb, Sn, Cu, Al and C. Coincidence measurements of neutrons [1] and fragments [2] were made with the same equipment shown in Fig. 2 of the report by Horváth et al. on page 99. The magnet deflected unreacted ^{6}He beam particles to a place (the E detectors) where neutrons produced as they stopped were not all directed at the neutron walls and where a shield could be interposed between them and the walls. The E detectors were 16 scintillator bars with PMTs at their ends.

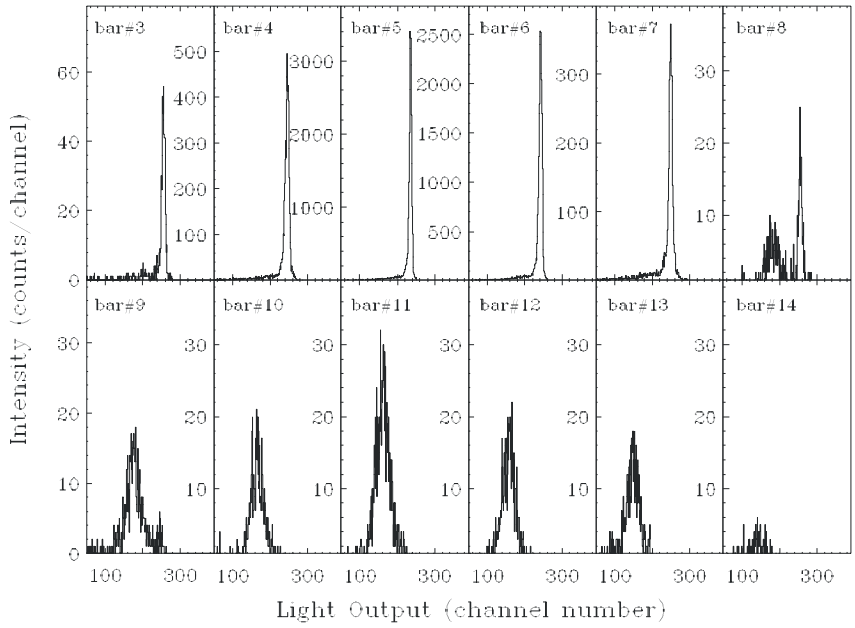

Fig. 1. Light output distributions in scintillator bars 3-14 for the U target. The sharp peak in Bars 3-8 are unreacted ^{6}He projectiles. The broad peak in Bars 8-14 are α-particles. Note the different intensity scales

Figure 1 shows the pulse height spectra in 12 of the 16 scintillator bars in coincidence with a neutron. The sharp peaks around channel 250 are from unreacted ^{6}He projectiles in accidental coincidence with neutrons. Most of these events are in Bars # 5 and 6. Coincidence with a neutron has reduced the number by almost a factor of 1,000. The bar number increases with deflection angle, and starting with Bar #8 we see the lower rigidity α-particles increase in intensity to a maximum in Bar #11 and then fall off. Kinematic spread in ^{6}He breakup is the main cause of the width of the α-particle peaks. It is easy to count the number of α-particles in spite of the fact that they are only ~ 10^{-4} of the particles entering the magnetic field.

σ_{-2n}, nuclear & Coulomb

From the integrated α-particle counts in Bars 8-14 and ^{6}He counts in Bars 3-8 we determined the relative values of σ_{-2n}. To get absolute values, we normalized the Al value to σ_{-2n} of ^{6}He on Si measured by Warner et al. [3] to be 0.46 ± 0.06b. All of the σ_{-2n} values are shown in Fig. 2. To extract the Coulomb parts we used the expected nuclear and Coulomb dependencies on A and Z,

$$\sigma_{-2n} = \sigma_{nuclear} + \sigma_{coulomb} = a(1.2A^{1/3} + 2.6) + bZ^{1.8}, \qquad (1)$$

and made the least-squares fit shown in the figure. For U and Pb the Coulomb part accounts for more than half of the total 2-n removal cross section of ^{6}He**.**

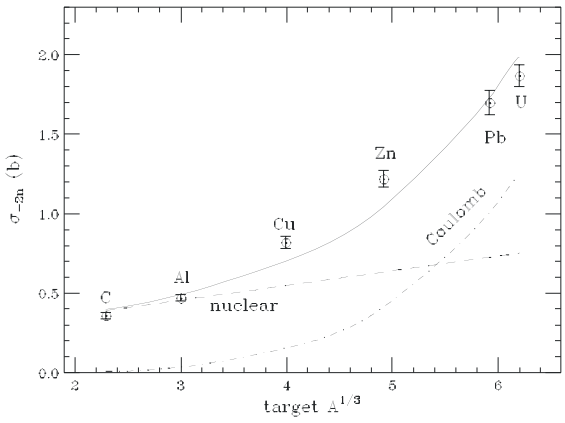

Fig. 2. Total 2n removal cross sections for the six targets. Points are the experimental data. Solid curve is a fitting model to extract the Coulomb part of the cross section, as in Eq. 1.

$P_{\|}$ Distributions & halo radius

The parallel momentum distributions for neutrons and α-particles are all well fitted by Gaussians. Figure 3 shows the σ values of the Gaussians plotted against the Z of the target. It can be observed that the

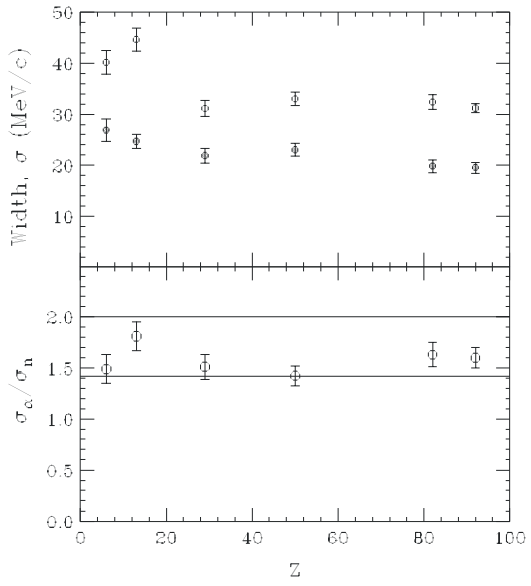

Fig. 3. (top) Widths of α-particle (open points) and neutron (filled points) parallel momentum distributions for the six targets. (bottom) Ratio of the above widths compared to $\sqrt{2}$ and to 2.0.

widths of both the neutron and the α-particle distributions decrease with the size of the target. The decrease may be attributed to the breakdown of the sudden approximation when the long-range Coulomb interaction

makes a significant contribution to the breakup. Theα-particle distribution obtained with the C target should most reliably give the distribution within ^{6}He. The width σ = 40.2±2.3 MeV/c of this momentum distribution determines the rms radius of its Fourier transfom space distribution $\langle r^2 \rangle^{-}$ = 2.95 ± 0.17 fm. The rms radius of the entire neutron matter distribution has been determined from ^{6}He interaction cross sections to be 2.59±0.04 fm [4] and 2.61±0.03 fm [5]. Our value for the halo neutrons alone is larger by 0.35± 0.17 fm.

Correlation of the halo neutrons

If the two halo neutrons in ^{6}He are correlated in their motion, for example, by having the same space coordinates or by sitting on opposite sides of the α-particle, sudden dissociation of ^{6}He will send the α-particle in one direction and the two neutrons in the opposite direction. In either of these "dineutron" pictures the angle θ_{nn} between the neutrons will be zero. We have two methods, using independent sets of data, with which to look for a correlation.

One method applies conservation of momentum to the momentum distributions of the preceding section. Conservation of momentum requires the momentum of the α-particle in ^{6}He to be balanced by the momentum of the two neutrons. It follows then that the widths of the α-particle and neutron distributions should be related. Applying the law of cosines to the triangle formed by the three momentum vectors gives

$$2\mathbf{p(n_1)\bullet p(n_2)} = p_{\_}^{\,2} - [p_{n1}^{\,2} + p_{n2}^{\,2}]. \qquad (2)$$

Averaging and noting that Gaussians have $\langle p_x^2 \rangle = \langle p_y^2 \rangle = \langle p_z^2 \rangle = \sigma^2$ so that $\langle p^2 \rangle = 3\sigma^2$ gives

$$\langle \mathbf{p(n_1)\bullet p(n_2)} \rangle = 1.5(\sigma_{\alpha\_}^{\,2} - 2\sigma_n^{\,2}). \qquad (3)$$

We use Eq. 3 for two special cases: Case 1. If the two neutrons are a dineutron, $\mathbf{p(n_1) = p(n_2)}$, the left side becomes $\langle p_n^2 \rangle = 3\sigma_n^2$, and $\sigma_{\alpha\_} = 2\sigma_n$. Case 2. If the two neutrons are not correlated, then $\langle \vec{p}(n_1)\vec{p}(n_2) \rangle = 0$, and $\sigma_{\alpha\_} = \sqrt{2}\sigma_n$. The values of $\sigma_{\alpha\_}/\sigma_n$ for the six targets and for the two special cases are shown in Fig. 3b. Case 1, where θ_{nn} = 0, and $\sigma_{\alpha\_}/\sigma_n$ = 2, is not supported by Fig. 3b. The data fluctuate near, but not around, the uncorrelated value, √2. So the halo neutrons are not completely uncorrelated.

In the other method we look directly at the θ_{nn}, or the $\cos(\theta_{nn})$, distribution function**.** The events in this set are sparse since each event has an α-n-n triple coincidence. The measured $\cos(\theta_{nn})$ distribution functions for the six targets are statistically equivalent. To reduce the fluctuations we summed the distributions, and that sum is shown in Fig. 4. The response of the detection system distorts the true $\cos\theta_{nn}$

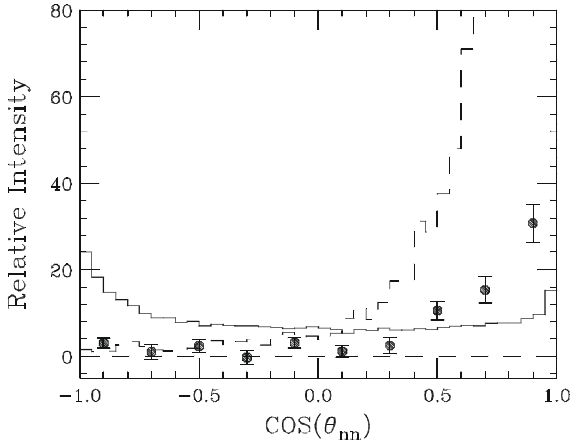

Fig. 4. Distribution of angle between the two neutrons from ^{6}He breakup. Points are from 2n-α coincidence events for the six targets used in the experiment. The angle was calculated in the 2n + α center-of-mass frame. Histograms result from Monte-Carlo simulations—solid: 3-bodyphase space model, dashed: dineutron model.

distribution. For example, the solid-angle acceptance of the system favors breakups with small values of θ_{nn}. To take that response and other geometry effects into account in comparing two theoretical models with experiment, we folded those effects with each theoretical $\cos(\theta_{nn})$ distribution in a Monte-Carlo simulation. The dashed histogram in Fig. 4, which is for the dineutron model, is strongly forward peaked; without the detector response it would be a delta function at $\cos(\theta_{nn}) = 1$. The solid histogram in Fig. 4 is for the 3-body phase space model. This model is meant to give the opposite extreme, where the two neutrons are uncorrelated. In fact, momentum conservation and α-particle recoil force a correlation in which the average value of $\cos(\theta_{nn})$ is somewhat less than 90˚ [6]. (In this model $\sigma_{\alpha\_}/\sigma_n < \sqrt{2}$) As in Fig. 3b for $\sigma_{\alpha\_}/\sigma_n$, the dineutron model is not favored by the $\cos(\theta_{nn})$ data of Fig. 4, but there is tendency towards it. This may be evidence for the hybrid model [7], a model in which the two valence neutrons of ^{6}He stay in shell model orbits when they are close to the core, but form a cluster (dineutron) when they are far from the core. If the ^{6}He nucleus breaks up when the neutrons are far from the core, the neutrons tend to be strongly correlated. If the ^{6}He breaks up when the neutrons are close to the core, the neutrons tend to be uncorrelated.

Dipole strength function

On the first page of this report we saw that with targets of Pb and U most of the 2-n removal cross section of ^{6}He is Coulomb induced. For each such event the final-state kinematics gave us the decay energy E_d and, therefore, the energy of the photon absorbed, resulting in some information on the dipole strength function $dB(E1)/dE_x$ through the following relation [8] to the measurable spectral function $d\sigma_{E1}/dE_d$.

$$\frac{dB(E1)}{dE_d} = \frac{9\hbar c}{16\pi^3}\frac{1}{n_{E1}(E_\gamma)}\frac{d\sigma_{E1}}{dE_d} \quad \text{.....(4)}$$

In this equation $E_\gamma = E_x = S_{2n} + E_d$, and $n_{E1}(E_\gamma)$ is the number of equivalent E1 photons with energy E_γ surrounding the target nucleus. For ^{6}He the value of S_{2n} is 0.975 MeV. The function $d\sigma_{E1}/dE_d$ differs from the measured spectral function in two respects. The measured function contains distortions introduced by the detection system, and it contains both Coulomb and nuclear contributions. In computer simulations using the detector response function, the distortions were removed. Figure 2 shows that for the U target 2/3 of σ_{-2n}, or 1.25 b, is Coulomb induced. We used this value to normalize the dipole strength function determined with the U target, and we assumed that the shape of the function was not significantly altered by the nuclear part. The result is shown in Fig. 5, where the shaded area gives the range allowed by the statistical uncertainty in. The function agrees with that determined by Aumann et al. [9] using ^{6}He at 240 MeV/nucleon.The dashed curve [10] in Fig. 5. comes from a 3-body model [11] based on hyperspherical harmonics and the coordinate-space Faddeev approach. The dot-dashed curve was derived from a model [12] in which $dB(E1)/dE_x$ is derived from the E1 strength function for one-neutron halo nuclei [13]. The experiment and the calculations agree that there is a strong concentration of E1 strength at low energy, $E_d \sim 1 - 2.5$ MeV.

a. Eötvös Loránd University, Budapest, Hungary
b. Rikkyo University, Tokyo, Japan
c. University of Notre Dame
d. CEFET, Curitiba, Pr, Brazil
e. KFKI, Hungary
f. Oberlin College, Oberlin, Ohio

Present Addresses
1. American Express, 200 Vesey St., New York, NY
2. Nat'l. Inst. Radiological Sciences, Chiba, Japan

3. Mayo Clinic, Rochester, MN
4. Investor Analytics LLC, 80 Broad Street, New York

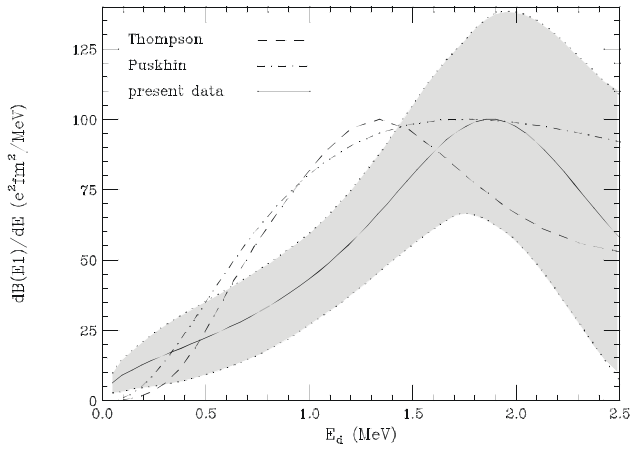

Fig. 5. Dipole strength function. Shaded area determined from the U data. Dashed curve [10, 11] and dot-dashed [12, 13] model predictions, both normalized to the experimental function.

References

1. P.D. Zecher, A. Galonsky, J.H. Kruse, S.J. Gaff, J. Ottarson, J. Wang, F. Deák, Á. Horváth, Á. Kiss, Z. Seres, K. Ieki, Y. Iwata and H. Schelin, Nucl. Instr. and Meth. **A401**, 329 (1997).
2. J.J. Kruse, A. Galonsky, C. Snow, E. Tryggestad, J. Wang[2], K. Ieki[*], Y. Iwata[*,3] and P.D. Zecher[4] NIM A, (2001).
3. R. E. Warner, R. A. Patty, P. M. Voyles, A. Nadasen, F. D. Becchetti, J. A. Brown, H. Esbensen, A. Galonsky, J. J. Kolata, J. Kruse, M. Y. Lee, R. M. Ronningen, P. Schwandt, J. von Schwarzenberg, B. M. Sherrill, K. Subotic, J. Wang, and P. Zecher, Phys. Rev. C **54**, 1700–1709 (1996).
4. I. Tanihata, D. Hirata, T. Kobyashi, S. Shimoura, K. Sugimoto and H. Toki, Phys. Lett. B **289**, 261 (1992).
5. A. Pushkin, B. Jonson and M.V. Zhukov, J. Phys. G: Nucl. Part. Phys. **22**, L95 (1996).
6. D. Sackett, K. Ieki, A. Galonsky, C.A. Bertulani, J.J. Kruse, W.G. Lynch, D.J. Morrissey, N.A. Orr, H. Schulz, B.M. Sherrill. A. Sustich, J.A. Winger, F. Deak, A. Horvath, A. Kiss, Z. Seres, J.J. Kolata, R.E. Warner, and D.L. Humphrey, Phys. Rev. C **48**, 118 (1993), pp. 132-3.
7. Kiyomi Ikeda, Nucl. Phys. **A538**, 355c (1992).
8. Carlos A. Bertulani and Gerhard Baur, Physics Reports 163, 299 (1988).
9. T. Aumann et al., Phys. Rev. C **59**, 1252 (1999).
10. Ian Thompson, private communication.
11. B.V. Danilin, M.V. Zhukov, J.S. Vaagen and J.M. Bang, Phys. Lett. B **302**, 129 (1993).
12. A. Pushkin, J. Phys. G: Nucl. Part. Phys. **22**, L95 (1996).
13. C.A. Bertulani and G. Baur, Nucl. Phys. **A480** 615 (1988).